

Geometric entanglement from matrix product state representations

Bing-Quan Hu, Xi-Jing Liu, Jin-Hua Liu and Huan-Qiang Zhou¹

¹Centre for Modern Physics and Department of Physics,
Chongqing University, Chongqing 400044, The People's Republic of China

An efficient scheme to compute the geometric entanglement per lattice site for quantum many-body systems on a periodic finite-size chain is proposed in the context of a tensor network algorithm based on the matrix product state representations. It is systematically tested for three prototypical critical quantum spin chains, which belong to the same Ising universality class. The simulation results lend strong support to the previous claim [Q.-Q. Shi, R. Orús, J. O. Fjærstad, and H.-Q. Zhou, New J. Phys **12**, 025008 (2010); J.-M. Stéphan, G. Misguich, and F. Alet, Phys. Rev. B **82**, 180406R (2010)] that the leading finite-size correction to the geometric entanglement per lattice site is universal, with its remarkable connection to the celebrated Affleck-Ludwig boundary entropy corresponding to a conformally invariant boundary condition.

PACS numbers: 03.67.-a, 03.65.Ud, 03.67.Hk

Introduction. In the last decade, significant progress has been made in the investigation of quantum phase transitions (QPTs) from a novel perspective-quantum entanglement [1]. The main idea is to quantify entanglement present in a ground-state wave function for a quantum many-body lattice system in terms of a variety of bipartite entanglement measures, with some anomaly at a critical point. A remarkable result is achieved for the von Neumann entropy that quantifies the bipartite entanglement when a finite-size spin chain is partitioned into two disjoint parts: it scales logarithmically with the subsystem's size, with a prefactor proportional to the central charge, a fundamental quantity in conformal field theory, as long as the system is at criticality [2–5].

Contrary to bipartite entanglement measures, no consensus has been achieved regarding multipartite entanglement measures, although much effort has been devoted to characterize quantum criticality from some multipartite entanglement measures. One promising candidate among them is the geometric entanglement (GE) [6, 7]. As a holistic measure of the multipartite entanglement, the GE quantifies the multipartite entanglement present in a quantum state wave function. For a quantum many-body lattice system, the GE per lattice site is shown to be an alternative way to detect critical points [7–11].

In addition, an intriguing connection between the GE per site and the Affleck-Ludwig g factor [12] is established for a finite-size spin chain with the periodic boundary conditions at criticality. More precisely, the GE per site, \mathcal{E}_N , scales as

$$\mathcal{E}_N \sim \mathcal{E}_\infty + \frac{b}{N} + O\left(\frac{1}{N^2}\right), \quad (1)$$

with N being the lattice size. It was conjectured that the coefficient b in the subleading term is universal [13]. This is confirmed later in Ref. [14] for both the transverse Ising and XXZ chains at criticality, by relating the coefficient b to the Affleck-Ludwig boundary entropy s :

$$b = -\frac{2}{\ln 2} s. \quad (2)$$

Here, the boundary entropy s is defined through the Affleck-Ludwig g factor: $s = \ln g$ [2–5]. This result is surprising,

in the sense that the Affleck-Ludwig boundary entropy s appears in the GE per lattice site for a *periodic* chain. However, it still remains unclear as to whether or not such a connection between the GE per site and the Affleck-Ludwig g factor is universally valid, and whether or not there is any criterion to judge which g factor, corresponding to a conformally invariant boundary condition, is chosen for a specific model. Therefore, it is desirable to investigate the models belonging to the same universality class, to see if the same g factor appears, thus providing further insights into the connection between the subleading term coefficient b in the GE per lattice site and the Affleck-Ludwig g factor.

One of the main obstacles to address these issues is due to the fact that the computation of the GE per lattice site is a formidable task for a quantum many-body lattice system, because it involves the optimization over all the possible separable states, with possibly some constraints arising from the translational invariance. However, recent progress in the context of the tensor network algorithms for quantum many-body lattice systems with the periodic boundary conditions [15–19] offers us an efficient method to systematically evaluate the GE per lattice site for quantum many-body lattice systems. In this paper, we first describe how to evaluate the GE per lattice site for a finite-size quantum spin chain from a tensor network algorithm based on the matrix product state representations. Then we present our simulation results for three prototypical spin chains belonging to the Ising universality class.

The geometric entanglement per lattice site. We first introduce the maximum fidelity Λ_{\max} between a quantum pure state $|\psi\rangle$ and all the possible separable and normalized states $|\phi\rangle$ of the N parties:

$$\Lambda_{\max} = \max_{|\phi\rangle} |\langle\phi|\psi\rangle|. \quad (3)$$

The larger Λ_{\max} is, the closer a quantum state wave function is to a separable state. Therefore, a holistic measure of the multipartite entanglement present in a quantum state wave function $|\psi\rangle$ is defined as

$$E(|\psi\rangle) = -\log_2 \Lambda_{\max}^2. \quad (4)$$

Since the contribution to $E(\psi)$ from each party is additive, $E(\psi)$ scales linearly with N , for a multipartite system consisting of N parties. Therefore, it is convenient to define the GE per party as

$$\mathcal{E}_N(|\psi\rangle) = N^{-1}E(|\psi\rangle). \quad (5)$$

For a quantum many-body lattice spin system, each lattice site constitutes a party. Thus, \mathcal{E}_N is the GE per lattice site. Note that it is well defined even in the thermodynamic limit.

A matrix product state algorithm. Let us recall the key steps to produce a ground-state wave function from an efficient variational algorithm [17] for a translational-invariant finite-size periodic lattice system. First, choose a random state as an initial state $|\psi_0\rangle$. Second, perform the imaginary time evolution for $|\psi_0\rangle$. Thus, we get the evolved state $|\psi_\tau\rangle$ at imaginary time τ ,

$$|\psi_\tau\rangle = \frac{\exp(-H\tau)|\psi_0\rangle}{\|\exp(-H\tau)|\psi_0\rangle\|}. \quad (6)$$

If $\tau \rightarrow \infty$, the ground-state wave function is projected out, as long as the initial state is not orthogonal to the real ground state. Third, exploit the Trotter-Suzuki decomposition and turn the imaginary time evolution operator into a series of two-site gates over a time slice $\delta\tau$, with $\tau = M\delta\tau$. Therefore, the problem becomes how to absorb a two-site gate acted on a matrix product state. For a periodic spin chain with N sites, we assume the matrix product state representation is translation-invariant under two-site shifts. Thus we only need two three-index tensors, A_o and A_e (cf. Fig. 1 (i)), to represent a tensor network for the ground-state wave function and two one-index tensors, B_o and B_e (cf. Fig. 1 (i)), to represent a separable state, as shown in Fig. 1 (ii) and (iii), respectively. Here, the subscripts o and e represent odd and even sites, respectively. In this setting, a two-site gate is absorbed by performing a singular value decomposition for a matrix contracted from a few tensors involving the two-site gate.

A peculiar feature of the algorithm for a finite-size periodic system is to take account of the p largest eigenvalues and the corresponding eigenvectors of the transfer matrix $E_{\langle\psi|\psi\rangle}$, when one evaluates the ground-state energy per site. That is, $E_{\langle\psi|\psi\rangle}^m = \sum_{i=1}^{D^2} u_i s_i^m v_i \approx \sum_{i=1}^p u_i s_i^m v_i$, where s_i is the i -th largest eigenvalue, u_i and v_i indicate the left and right eigenvectors, respectively, with D denoting the bond dimension. When the energy per site converges, the ground-state wave function is generated. Note that the computational cost of the algorithm is pD^3 .

The geometric entanglement per lattice site from matrix product state representations. Now we are ready to compute the GE per lattice site. The crucial step is how to maximize the fidelity $|\langle\phi|\psi\rangle|$ over all the possible separable states $|\phi\rangle$. In Fig. 1 (iv), we introduce the transfer matrix $E_{\langle\phi|\psi\rangle}$ to represent the fidelity between $|\psi\rangle$ and $|\phi\rangle$, with $E_{\langle\phi|\psi\rangle}$ constructed from two three-index tensors, A_o and A_e , and two one-index tensors, B_o^* and B_e^* . Mathematically, the fidelity between a

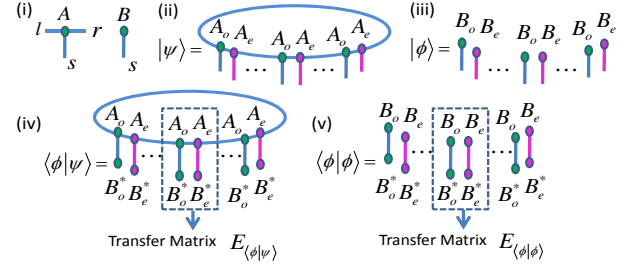


FIG. 1: (color online) (i) Two three-index tensors A_o^{lrs} and A_e^{lrs} are attached to odd and even sites respectively, to represent a ground-state wave function. Two one-index tensors B_o^s and B_e^s , attached to odd and even sites respectively, represent a separable state. Here, s is the physical index, l and r are the inner bond indices. (ii) The pictorial representation for a ground-state wave function $|\psi\rangle$. (iii) The tensor network representation for a separable state $|\phi\rangle$. (iv) The fidelity between the ground-state wave function $|\psi\rangle$ and a separable state $|\phi\rangle$. The transfer matrix $E_{\langle\phi|\psi\rangle}$ for the fidelity is constructed from the tensors A_o , A_e , B_o^* and B_e^* . (v) The norm for a separable state $|\phi\rangle$, where the transfer matrix $E_{\langle\phi|\phi\rangle}$ is constructed from B_o , B_e , and their conjugates.

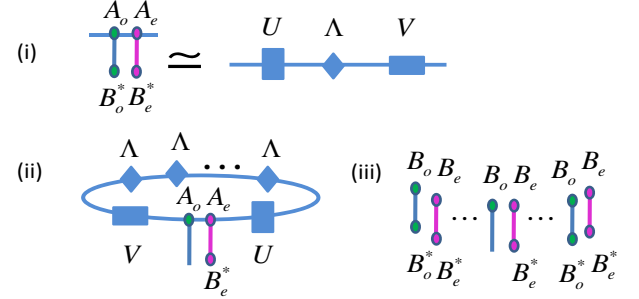


FIG. 2: (color online) (i) The transfer matrix $E_{\langle\phi|\psi\rangle}$ may be approximated by the p largest eigenvalues Λ and the corresponding left and right eigenvectors, U and V , of the transfer matrix $E_{\langle\phi|\psi\rangle}$. (ii) The pictorial representation for the derivative of $\langle\phi|\psi\rangle$ with respect to B_o^* . (iii) The pictorial representation for the derivative of $\langle\phi|\phi\rangle$ with respect to B_o^* .

ground-state wave function $|\psi\rangle$ and a separable state $|\phi\rangle$ is expressed as:

$$f = \frac{|\langle\phi|\psi\rangle|}{\sqrt{\langle\psi|\psi\rangle\langle\phi|\phi\rangle}}. \quad (7)$$

For our purpose, we consider $F = f^2$ instead of f itself. To maximize F , we compute its logarithmic gradient with respect to a one-index tensor B^* ,

$$\frac{\partial \ln F}{\partial B^*} = \frac{1}{\langle\phi|\psi\rangle} \frac{\partial \langle\phi|\psi\rangle}{\partial B^*} - \frac{1}{\langle\phi|\phi\rangle} \frac{\partial \langle\phi|\phi\rangle}{\partial B^*}. \quad (8)$$

Here, B^* is either B_o^* or B_e^* . We take B_o^* as an example to explain the updating procedure. The pictorial representation for the derivative of $\ln F$ with respect to B_o^* is shown in Fig. 2. In Fig. 2(i), $E_{\langle\phi|\psi\rangle}$ is approximated by the first p largest eigenvalues and the corresponding eigenvectors of $E_{\langle\phi|\psi\rangle}$. That implies that $E_{\langle\phi|\psi\rangle}^m \approx \sum_{k=1}^p U_k \Lambda_{k,k}^m V_k$, with p specifically depending on

m : the larger m is, the less p is. In Fig. 2(ii), the derivative of $\langle\phi|\psi\rangle$ with respect to B_o^* is shown. In Fig. 2(iii), we represent the derivative of $\langle\phi|\phi\rangle$ with respect to B_o^* . Once the fidelity gradient is determined, the real and imaginary parts of B_o may be updated as follows:

$$\Re B_o = \Re B_o + \delta \Re(\frac{\partial F}{\partial B_o}), \quad (9a)$$

and

$$\Im B_o = \Im B_o + \delta \Im(\frac{\partial F}{\partial B_o}), \quad (9b)$$

where δ is the step size in the parameter space, which is tuned to be decreasing during the updating procedure. Here, we have normalized the tensors B_o , $\Re(\partial F/\partial B_o)$ and $\Im(\partial F/\partial B_o)$ by setting their respective largest entries to be unity. In exactly the same way, we may update the other tensor B_e . Repeating the procedure until the fidelity per lattice site converges, we achieve the closest separable state $|\phi\rangle$ that ensures its maximum fidelity with the ground-state wave function $|\psi\rangle$. Thus, the GE per lattice site follows, as desired.

The models. We test our scheme by considering three prototypical critical quantum spin chains with the periodic boundary conditions. Note that the models belong to the same Ising universality class.

The first model is quantum Ising model in a transverse magnetic field on a finite-size ring. The Hamiltonian takes the form:

$$H = - \sum_{i=1}^N (\sigma_x^{[i]} \sigma_x^{[i+1]} + \lambda \sigma_z^{[i]}), \quad (10)$$

where $\sigma_\alpha^{[i]}$ ($\alpha = x, z$) are the Pauli spin operators at site i , and λ is a transverse magnetic field. The model is critical at $\lambda_c = 1$.

The second model is a spin-1/2 Ising chain with antisymmetric anisotropic and alternative bond interactions. It is described by the Hamiltonian:

$$H = \sum_{i=1}^N ((1 - (-1)^i r) \sigma_z^{[i]} \sigma_z^{[i+1]} + D_z (\sigma_x^{[i]} \sigma_y^{[i+1]} - \sigma_y^{[i]} \sigma_x^{[i+1]})), \quad (11)$$

where $\sigma_\alpha^{[i]}$ ($\alpha = x, y, z$) are the Pauli spin-1/2 operators at site i . The alternative bond interaction is characterized by the relative strength r of the exchange coupling, and D_z is the z direction component of the Dzyaloshinskii-Moriya interaction arising from the spin-orbit coupling. The model is critical at $D_z \sim 0.263$, if r is chosen to be 0.5 [20].

The third model is quantum XYX model in an external magnetic field described by the Hamiltonian:

$$H = \sum_{i=1}^N (\sigma_x^{[i]} \sigma_x^{[i+1]} + \Delta_y \sigma_y^{[i]} \sigma_y^{[i+1]} + \sigma_z^{[i]} \sigma_z^{[i+1]} + h \sigma_z^{[i]}), \quad (12)$$

where $\sigma_\alpha^{[i]}$ ($\alpha = x, y, z$) are the Pauli operators at site i , Δ_y is a parameter describing the rotational anisotropy, and h is an

external magnetic field. For $\Delta_y = 0.25$, the critical magnetic field is $h_c = 3.206$ [21–23].

Simulation results. For the transverse Ising model, we have evaluated the GE per lattice site, as shown in Fig. 3(a), with $b = 1.016076$, consistent with our previous result in Ref. [13]. This yields the Affleck-Ludwig g factor $g = 0.7032$. Compared to the exact value $g_{\text{fixed}} = 1/\sqrt{2}$ [12], the relative error is $|(g - g_{\text{fixed}})|/g_{\text{fixed}} = 1.3 \times 10^{-4}$. We emphasize that, for this model, we have chosen the separable states to be translation-invariant under one-site shifts, although there is no a priori reason to argue that the GE per lattice site does not depend on the unit cell of the separable states under translational shifts. However, the same g factor is yielded, even if the separable states are translation-invariant under two-site shifts. In fact, we have evaluated the GE per site without *any* translation-invariant assumption, the same g factor is achieved. Thus, we conclude that *only* the smaller g factor, corresponding to the stable conformally invariant boundary condition [24], i.e., fixed boundary condition, is involved.

In Fig. 3(b), we plot the GE per lattice site, \mathcal{E}_N , as a function of the number of the lattice sites, N , for the spin-1/2 Ising chain with the coupling parameters $r = 0.5$ and $D_z = 0.263$. The finite-size scaling for the GE per lattice site follows $\mathcal{E}_N = a + b/N + f/N^2$, where the coefficients are $a = 0.083320$, $b = 0.966353$ and $f = -1.398155$. It yields the Affleck-Ludwig g factor $g = 0.715330$. Compared with the exact value $g_{\text{fixed}} = 1/\sqrt{2}$ [12] for the conformally invariant fixed boundary condition, the relative fitting error is $|(g - g_{\text{fixed}})|/g_{\text{fixed}} = 1.1 \times 10^{-2}$. For this model, we have chosen the separable states to be translation-invariant under two-site shifts, given the alternative bond interaction. However, we have evaluated the GE per site without *any* translation-invariant assumption, the same g factor is achieved. Thus, we conclude that *only* the smaller g factor, corresponding to the stable conformally invariant boundary condition [24], i.e., fixed boundary condition, is involved.

In Fig. 3(c), we plot the GE per lattice site, \mathcal{E}_N , as a function of the number of the lattice sites, N , for quantum XYX model in an external field, with $\Delta_y = 0.25$, where the size N is chosen from 10 to 100. Remarkably, it splits into two branches for a large enough chain size: one is for the separable states that are translation-invariant under one-site shifts, and the other is for the separable states that are translation-invariant under two-site shifts. The exact diagonalization for small-size chains up to 24 is also performed to evaluate the GE per site without *any* translation-invariant assumption. However, it only reproduces the second branch, as seen in Fig. 3(c). A proper explanation for this unexpected result is that, for this model, the translational invariance under one-site shifts constitutes a true constraint to separable states. That is, the closest separable state with the one-site unit cell is different from the closest separable state with the two-site unit cell. Thus the maximum fidelity Λ_{max} is larger for the latter, implying that the GE per lattice site is smaller, as long as the chain size is large enough. This explains the presence of a threshold in the chain size: the GE per site is the same for both

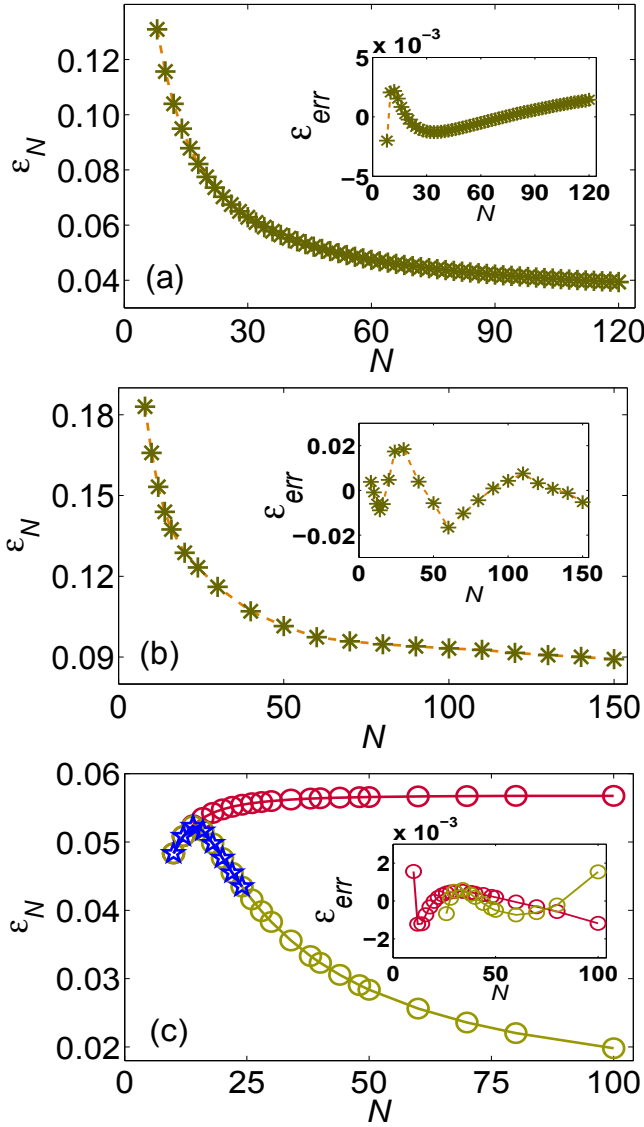


FIG. 3: (color online) Main: A scaling relation between the GE per lattice site ε_N and the chain size N , for quantum Ising model (a), with the size N ranging from 8 to 120, for quantum Ising model with antisymmetric anisotropic and alternative bond interactions (b), with the size N ranging from 8 to 150, and for quantum XYX model (c), with the size N ranging from 10 to 100. The data are fitted into $\varepsilon_N = a + b/N + f/N^2$, with $a = 0.030960$, $b = 1.016076$ and $f = -1.712521$ in (a) and $a = 0.083320$, $b = 0.966353$ and $f = -1.398155$ in (b). In (c), we have $a = 0.056892$, $b = 0.001581$, and $f = -0.879631$, and $a = 0.010193$, $b = 1.009600$ and $f = -5.005750$, respectively, for the upper and lower branches. Here, the upper (lower) branch is for the separable states that are translation-invariant under one-site (two-site) shifts, if the chain size is larger than a threshold. Indeed, the GE per site is the same for two cases, if the chain size is less than the threshold. In addition, the exact diagonalization results for the GE per lattice site are displayed in five-pointed stars, up to the chain size 24. The data match very well. Inset: The relative fitting error $\varepsilon_{err} = (\varepsilon_N^{\text{data}} - \varepsilon_N^{\text{fit}})/\varepsilon_N^{\text{fit}}$ are less than 2.1×10^{-3} in (a), less than 1.8×10^{-2} in (b), and less than 1.5×10^{-3} in (c), where $\varepsilon_N^{\text{fit}}$ is the value extracted from the fit and $\varepsilon_N^{\text{data}}$ is our simulation value for each N .

the one-site and two-site unit cells, if the size is less than the threshold. Two sets of the data are separately fitted into the scaling function $\varepsilon_N = a + b/N + f/N^2$, with the coefficients $a = 0.056892$, $b = 0.001581$, and $f = -0.879631$, and $a = 0.010193$, $b = 1.009600$ and $f = -5.005750$, respectively, yielding $g_{\text{XYX}} = 0.9994$ and $g_{\text{XYX}} = 0.7048$. They are consistent with the exact values $g_{\text{free}} = 1$ and $g_{\text{fixed}} = 1/\sqrt{2}$ [12] for conformally invariant free and fixed boundary conditions in the Ising universality class.

Summary. In this paper, we have developed a scheme to efficiently compute the GE per lattice site for quantum many-body spin systems on a periodic finite-size chain in the context of a tensor network algorithm based on the matrix product state representations. The computational cost does not depend on the chain size. A systematic test is performed for three prototypical critical quantum spin chains belonging to the same Ising universality class. The simulation results lend strong support to the previous claim that the leading finite-size correction to the GE per lattice site is universal [13], with its remarkable connection to the celebrated Affleck-Ludwig boundary entropy corresponding to a conformally invariant boundary condition [14]. For all the models tested, the simulated g is compared to the exact g factor from conformal field theory, with the relative error less than 1.1×10^{-2} . It appears that the boundary entropy corresponding to the smallest g factor is always involved. This is somewhat expected, since this g factor characterizes a stable fixed point along a boundary renormalization group flow, according to the Affleck-Ludwig g theorem [12]. Remarkably, for quantum XYX model in an external field, either conformally invariant free or fixed boundary condition appears, depending on the one- or two-site unit cell of the translation-invariant separable states.

Acknowledgements. We thank J.O. Fjærestad and R. Orús for their inspiring discussions. The work is partially supported by the National Natural Science Foundation of China (Grant No: 10874252). XJL and JHL are supported by the Fundamental Research Funds for the Central Universities (Project No. CDJXS11102213) and by Chongqing University Postgraduates' Science and Innovation Fund (Project No.: 200911C1A0060322).

-
- [1] L. Amico, R. Fazio, A. Osterloh, and V. Vedral, Rev. Mod. Phys. **80**, 517 (2008) and references therein.
 - [2] G. Vidal *et al.*, Phys. Rev. Lett. **90**, 227902 (2003).
 - [3] V.E. Korepin, Phys. Rev. Lett. **92**, 096402 (2004).
 - [4] P. Calabrese and J. Cardy, J. Stat. Mech. P06002 (2004).
 - [5] H.-Q. Zhou, T. Barthel, J.O. Fjærestad, and U. Schollwöck, Phys. Rev. A **74**, 050305(R) (2006).
 - [6] H. Barnum and N. Linden, J. Phys. A: Math. Gen. **34**, 6787 (2001).
 - [7] T.-C. Wei and P. M. Goldbart, Phys. Rev. A **68**, 042307 (2003); T.-C. Wei, D. Das, S. Mukhopadhyay, S. Vishveshwara, and P.M. Goldbart, Phys. Rev. A **71**, 060305 (2005).
 - [8] A. Botero and B. Reznik, arXiv:0708.3391; R. Orús, Phys. Rev. Lett. **100**, 130502 (2008).

- [9] R. Orús and T.-C. Wei, Phys. Rev. B **82**, 155120 (2010).
- [10] R. Orús, T.-C. Wei, and H.-H. Tu, arXiv:1010.5029; R. Orús and T.-C. Wei, arXiv:1006.5584.
- [11] C.-Y. Huang and F.-L. Lin, Phys. Rev. A **81**, 032304 (2010).
- [12] I. Affleck and A. W. W. Ludwig, Phys. Rev. Lett. **67**, 161 (1991).
- [13] Q.-Q. Shi, R. Orús, J.O. Fjærestad, and H.-Q. Zhou, New J. Phys **12**, 025008 (2010).
- [14] J.-M. Stéphan, G. Misguich, and F. Alet, Phys. Rev. B **82**, 180406R (2010).
- [15] F. Verstraete, D. Porras, and J. I. Cirac, Phys. Rev. Lett. **93**, 227205 (2004).
- [16] P. Pippin, S. R. White, and H. G. Evertz, Phys. Rev. B **81**, 081103(R) (2010).
- [17] Q.-Q. Shi and H.-Q. Zhou, J. Phys. A: Math. Theor. **42**, 272002 (2009).
- [18] B. Pirvu, F. Verstraete, and G. Vidal, Phys. Rev. B **83**, 125104 (2011)
- [19] D. Rossini, V. Giovannetti, and R. Fazio, J. Stat. Mech. (2011) P05021.
- [20] B. Li, S. Y. Cho, H.-L. Wang, and B.-Q. Hu, arXiv:1105.0533 (2011).
- [21] J.-H. Zhao, H.-L. Wang, B. Li, and H.-Q. Zhou, Phys. Rev. E **82**, 061127 (2010).
- [22] J.-H. Liu, Q.-Q. Shi, H.-L. Wang, J. Links, and H.-Q. Zhou, arXiv:0909.3031 (2009).
- [23] J. Kurmann *et al.*, Physica A **112**, 235 (1982); D. V. Dmitriev *et. al.*, J. Exp. Theor. Phys. **95**, 538 (2002); T. Roscilde, *et. al.*, Phys. Rev. Lett. **93**, 167203 (2004).
- [24] J. L. Cardy, Nucl. Phys. B **240**, 514 (1984); Nucl. Phys. B **324**, 581 (1989).